Proc. Natl. Acad. Sci. USA
Vol. 93, pp. 4235–4239, April 1996
Neurobiology

Mixed synapses discovered and mapped throughout mammalian spinal cord

JOHN E. RASH*†‡§, ROBERT K. DILLMAN*†‡, BRENT L. BILHARTZ*, HEATHER S. DUFFY*†, L. RAY WHALEN*†, AND THOMAS YASUMURA*

*Department of Anatomy and Neurobiology, †Program in Neuronal Growth and Development, and ‡Program in Cell and Molecular Biology, Colorado State University, Fort Collins, CO 80523

Communicated by Thomas S. Reese, National Institutes of Health, Bethesda, MD, December 16, 1995 (received for review October 12, 1995)

ABSTRACT **Previously, synaptic activity in the spinal cord of adult mammals was attributed exclusively to chemical neurotransmission. In this study, evidence was obtained for the existence, relative abundance, and widespread distribution of "mixed" (chemical and electrical) synapses on neurons throughout the spinal cords of adult mammals. Using combined confocal microscopy and "grid-mapped freeze fracture," 36 mixed synapses containing 88 "micro" gap junctions (median = 45 connexons) were found and mapped to 33 interneurons and motor neurons in Rexed laminae III–IX in cervical, thoracic, and lumbosacral spinal cords of adult male and female rats. Gap junctions were adjacent to presumptive active zones, where even small gap junctions would be expected to increase synaptic efficacy. Two morphological types of mixed synapse were discerned. One type contained distinctive active zones consisting of "nested" concentric toroidal deformations of pre- and postsynaptic membranes, which, because of their unusual topology, were designated as "synaptic sombreros." A second type had gap junctions adjacent to active zones consisting of broad, flat, shallow indentations of the plasma membrane. Morphometric analysis indicates that mixed synapses correspond to 3–5% of all synapses on the somata and proximal dendrites, but, because of their subcellular location and morphology, they could represent 30–100% of excitatory synapses. The relative abundance of mixed synapses on several classes of neurons in spinal cords of adult rats suggests that mixed synapses provide important but previously unrecognized pathways for bidirectional communication between neurons in the mammalian central nervous system.**

Synapses, the specialized sites for rapid communication between neurons, are classified as chemical, electrical, or "mixed" (i.e., chemical plus electrical) (1–5). Of the three types, only chemical synapses are thought to occur widely in the mammalian central nervous system (2, 3, 6). In contrast, electrical synapses (7), although common in the spinal cords of lower vertebrates and in neonatal mammals (4, 8–11), are thought to be extremely rare in the spinal cords of adult mammals, having been found only in two small clusters of motor neurons that synchronize the contractions of ejaculatory muscles in adult male rats (12, 13). Mixed synapses, however, have not been observed previously in any region of the spinal cords of adult mammals (2, 3). Consequently, gap junctions have been suggested to represent an ontogenetically and phylogenetically "primitive" device for intercellular communication that has been all but abandoned between neurons in the central nervous system of adult mammals (2, 6). [Their apparent absence has been explained as providing a "mechanism to increase the metabolic and functional independence of neurons, in order to permit more complex information processing" (6).] However, recent demonstrations of widespread expression of several genes encoding for gap junction proteins in mammalian brain and spinal cord (reviewed in ref. 14) have revived suggestions that neuronal gap junctions are present but that they are too small to have been detected by use of conventional thin-section, immunocytochemical, or electrophysiological techniques (15–19). To address this issue, we developed "grid-mapped freeze fracture" (20), which has allowed us to discover very small gap junctions at ultrastructurally defined mixed synapses and to map their locations throughout the spinal cords of adult rats.

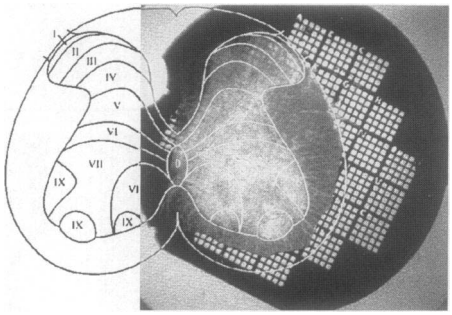

FIG. 1. Confocal image of freeze-fractured hemisection of adult rat spinal cord mounted in Lexan on a 3-mm-diameter gold "index" grid. Outlines indicate distinctive groups of neurons designated as the Rexed laminae (23). Dorsal horn (laminae I–V) is at top, and ventral horn (laminae VII–IX) is at bottom.

MATERIALS AND METHODS

Adult rats (six male and one female, 120–275 g) were anesthetized with ketamine (100 mg/kg) and xylazine (20 mg/kg) and fixed by transcardiac whole-body perfusion with 2.5% glutaraldehyde in 0.15 M Sorensen's phosphate buffer (pH 7.3–7.4) (21). Twenty-two transverse 100-μm-thick slices from lumbosacral and cervical enlargements and midthoracic segments of spinal cord were frozen, freeze-fractured, and replicated in JEOL freeze-etch devices (model nos. JFD 9000 or RFD 9010C) (22), and prepared by grid-mapped freeze fracture (20). After photographic mapping (Fig. 1) in a Molecular Dynamics Multiport 2001 inverted confocal laser scanning microscope, tissues were removed by digestion in 5.25% sodium hypochlorite, and the replicas were examined in a JEOL 2000 EX-II transmission electron microscope. Low- to high-magnification images (×50 to ×100,000) were photographed as stereoscopic pairs having an included angle of 8°. Locations of mixed synapses (seen in electron micrographs) were identified in corresponding confocal microscope images and plotted on standardized maps delineating distinctive layers of spinal cord neurons—i.e., the Rexed laminae (23), as subsequently refined (24) (Fig. 1, outlines).

Neurons were distinguished from glia based on published criteria (2, 3, 25, 26), including (*i*) somata >20 μm in diameter, (*ii*) nuclei >12 μm in diameter, (*iii*) cytoplasm with widely spaced (≈0.25 μm) parallel stacks of membranes (i.e., Nissl

The publication costs of this article were defrayed in part by page charge payment. This article must therefore be hereby marked "*advertisement*" in accordance with 18 U.S.C. §1734 solely to indicate this fact.

§To whom reprint requests should be addressed.

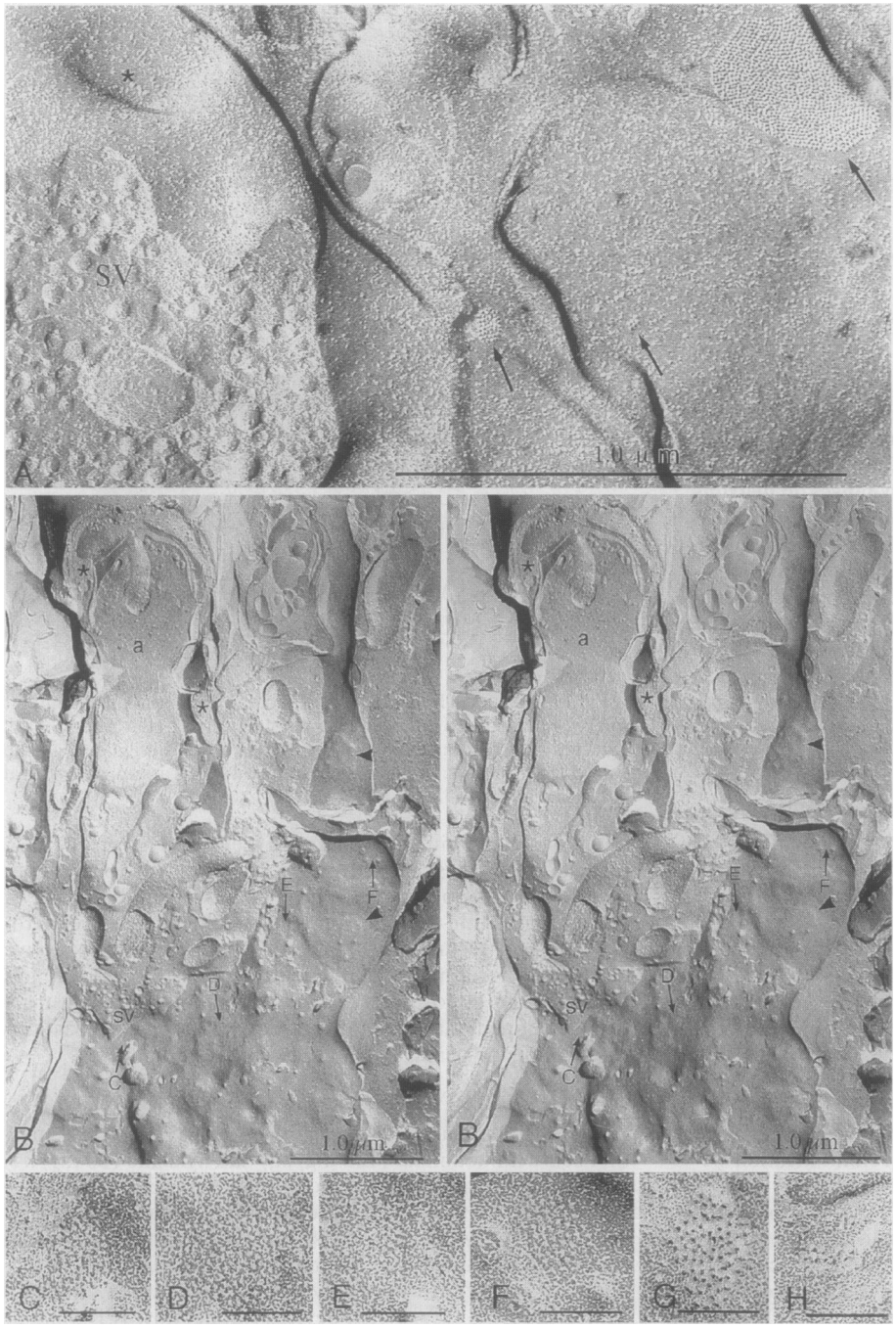

FIG. 2. Portions of mixed synapses from lumbosacral region of adult rat spinal cord. Uniform-diameter spherical synaptic vesicles (*A* and *B*) and cross-fractured and/or surface-fractured invaginations of the presynaptic membrane within or immediately adjacent to active zones (*B*) represent stages in exocytosis of synaptic vesicle and/or endocytosis of coated vesicles (27–29). (*A*) Mixed synapse having seven gap junctions (*A*, arrows), one with six connexons and one with 704 connexons (i.e., the largest and smallest found to date). Distinctive presynaptic impressions (*) may represent the P-face image of the "synaptic sombrero" as seen in Figs. 3 and 4. (*B*) Mixed synapse at axon terminal. Terminal loops of myelin (*) surround cross-fractured axoplasm (a). Distinctive flattened active zones (arrowheads) are interspersed with gap junctions (arrows E and F) and with circular profiles representing stages of exocytosis and endocytosis. (*C–F*) E-face images of gap junctions from *B* (arrows C–F). (*G* and *H*) Two P-face images of gap junctions from outside the imaging area in *B*. Variations in local shadowing angle affect image contrast and definition. (Bars = 0.1 μm, unless otherwise indicated.)

substance), (*iv*) more than five closely spaced synaptic contacts on somatic and proximal dendritic plasma membranes, and (*v*) plasma membranes containing distinctive clusters of subsynaptic intramembrane particles commonly called postsynaptic densities (3).

Chemical synapses were identified when they demonstrated three or more of the following: (*i*) apposition of synapse-like profiles on confirmed neuronal plasma membranes; (*ii*) presence of >25 uniform-diameter, closely packed, spherical synaptic vesicles in the putative presynaptic cytoplasm (Fig. 2*A*); (*iii*) presence of distinctive "active zones" (1, 3, 30) in the presynaptic membrane (Fig. 2*B*, arrowheads; Figs. 3*A* and 4*A*, synaptic sombreros); (*iv*) evidence of ongoing exocytosis at active zones, with endocytosis occurring in the surrounding presynaptic plasma membrane (3, 27–29) (Figs. 2*B*, 3*A*, and 4*A*); and (*v*) to identify axon telodendria, the presence of terminal loops of myelin demarcating the terminal Ranvier heminode (Fig. 2*B*).

Electron micrograph negatives at ×100,000 were scanned into a PowerMacintosh 8100 computer using a Leaf Lumina camera (Leaf Systems, Westborough, MA), and data regarding number of connexons per gap junction were analyzed using National Institutes of Health IMAGE 1.57. Statistical data were compiled and graphed using CA-CRICKET GRAPH 1.5.1 (Computer Associates, Islandia, NY). Digital images were "dodged" using Adobe PHOTOSHOP 2.5.1 and printed using a Kodak XLS 8300 digital printer.

RESULTS

In freeze-fracture replicas of cells identified as neurons (criteria listed in *Materials and Methods*), mixed synapses were identified by the dual presence of gap junctions (Fig. 2*A*, arrows) and morphological correlates of chemical synapses. Gap junctions were differentiated from other arrays of intramembrane particles and pits (for example, active zones and their associated postsynaptic densities) based on well-

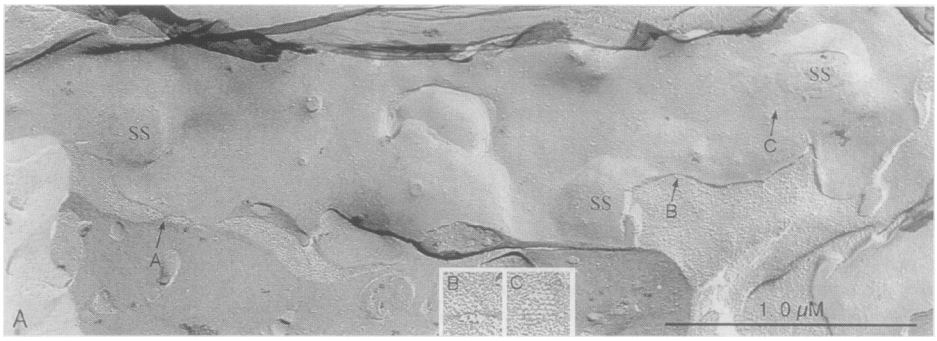

FIG. 3. (*A*) Mixed synapse with three active zones designated synaptic sombreros (SS), each with a gap junction (arrows A–C) in the "brim" of the sombrero. (*B* and *C*) Inset images show two of the gap junctions (B and C) at higher magnification. The third gap junction (A) is shown in Fig. 4*A*.

established criteria (22, 25–27, 30, 31), including (*i*) presence of 7- to 9-nm P-face intramembrane particles and/or E-face pits (32) in distinctive hexagonal arrays (Fig. 4 *A–D*); (*ii*) continuity of alignment of the hexagonal lattice of particles and pits where the fracture plane steps from P- to E-face (Fig. 4*C*); and (*iii*) narrowing of the extracellular space within the perimeter of gap junctions (Fig. 4 *A*, *C*, and *D*).

In several hundred small patches of plasma membranes, 36 mixed synapses (Fig. 2–4) containing a total of 88 gap junctions were identified. Moreover, all of the neuronal gap junctions were in mixed synapses (i.e., none were found in purely electrical synapses). Two-thirds (24 of 36) of the mixed synapses were on somata or proximal dendrites. Of the remaining mixed synapses, 10 (28%) were on small-diameter dendrites, and two (6%) were on small patches of plasma membrane (Fig. 4*D*), all at unknown distances from their respective neuronal somata.

Mixed synapses in spinal cord consisted of two morphological types. Almost half (17 of 36) contained active zones consisting of "nested" (i.e., parallel-stacked pre- and postsynaptic) membrane deformations that we call synaptic sombreros (Figs. 3*A* and 4*A*) because of their distinctive topology as seen in stereoscopic images (Fig. 4*A*). In 17 mixed synapses, 44 synaptic sombreros (average = 2.6 per synapse) were discerned, usually with a small gap junction near or within the brim of each sombrero (Figs. 3*A*; 4*A*, arrows; and 5*A*). In an apparent second type of mixed synapse (n = 19), synaptic sombreros were not present, but active zones consisting of broad, shallow indentations of the nerve terminal plasma membrane (synaptic mesas) were observed (Figs. 2*B*, arrowheads; and 5*B*). Synaptic vesicle exocytosis occurred within both types of active zones, often near the margins of gap junctions (Figs. 2 *B–E*), whereas additional exocytosis and/or endocytosis occurred in the surrounding nerve terminal plasma membrane (Figs. 2*B*, 3*A*, 4*A*, and 5). Although the significance of two possible morphological types of mixed synapses is unknown, the distinctive morphology of synaptic sombreros, in particular, and the presence of spherical synaptic vesicles may aid in identifying the neurotransmitter(s) involved (33), presumably as a necessary step in determining the function(s) of mixed synapses.

In most spinal cord mixed synapses, several gap junctions were present (Figs. 2*A* and 3*A*). Of all gap junctions found in spinal cord neurons, 75 were present in 23 clusters, consisting of 2–6 gap junctions per cluster (average = 3.3 gap junctions per cluster). With all data combined (88 gap junctions in 36 mixed synapses), there were 2.4 gap junctions per mixed synapse. Because 10 of the remaining 13 single gap junctions were present at fracture edges (Fig. 4 *A* and *D*) or in fragments of synaptic contacts that were too small to include entire clusters (Fig. 4*D*), it is likely that several of those mixed synapses contained additional gap junctions that were not exposed by the fracture plane. Regardless, multiple gap junctions occur in most mixed synapses in adult rat spinal cord.

Compared with gap junctions in other tissues, which often contain several thousand to as many as 100,000 connexons (34), the number of gap junctions in rat spinal cord mixed synapses was unusually small; the median number of connexons was 45 (Fig. 6). Even by comparison with gap junctions in electrical synapses from the sexually dimorphic motor nuclei (12, 13), gap junctions in spinal cord mixed synapses contained only about one-sixth as many connexons (G. Zampighi, per-

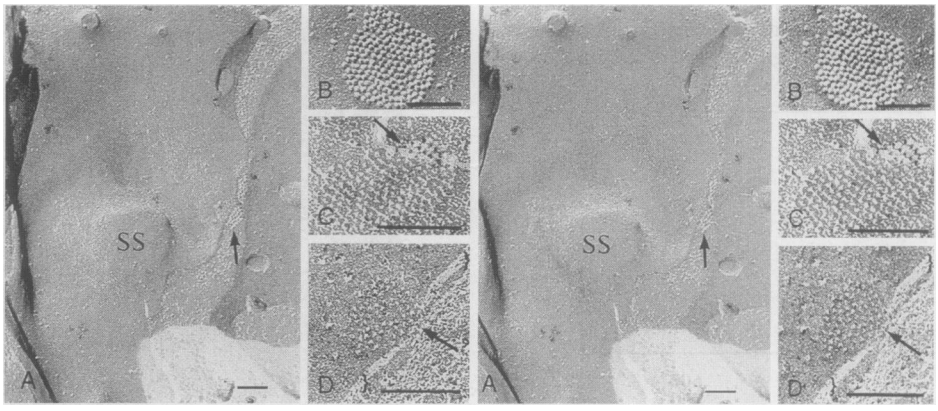

FIG. 4. (*A*) Higher magnification stereoscopic image of one of three synaptic sombreros from Fig. 3. Note the distinctive raised central "crown" and equally distinctive surrounding brim. Within the brim is an irregular gap junction. (*B–D*) Gap junctions are defined by the presence of 7- to 9-nm P-face particles and/or E-face pits in distinctive hexagonal arrays (*B* and *C*), continuity of alignment of the rows of particles and pits where the fracture plane steps from P- to E-face (*C*, arrow), and distinctive narrowing of the extracellular space within the perimeter of gap junctions (*D*, arrow).

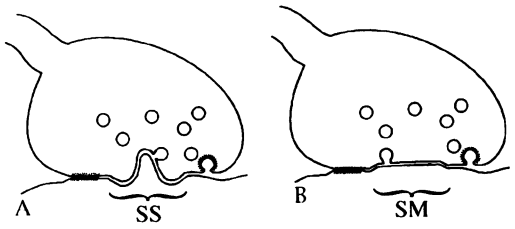

FIG. 5. Drawings of two types of mixed synapses, one with deeply invaginated active zones called synaptic sombreros (*A*) and one with broader, flatter active zones ("synaptic mesas") (*B*). Gap junctions are often observed near exocytotic/endocytotic profiles (*B*).

sonal communication). Moreover, because most gap junctions in spinal cord mixed synapses were smaller than the thickness of conventional thin sections (i.e., <0.07 μm in diameter), most would not be resolvable by conventional thin-sectioning methods (for rationale, see refs. 12 and 13).

Mixed synapses in spinal cord were found on both interneurons and motor neurons, as identified based on cell diameter and location of the somata within the Rexed laminae (23, 24) (see Fig. 1). Moreover, they were found on neurons in laminae III–IX, including laminae IV–IX in the lumbosacral enlargement (Fig. 7); on laminae VI, VII, and IX in the cervical enlargement (not shown); and in lamina III and at the margins of laminae VI and VII in the thoracic region (not shown). Because only interneurons have their somata in laminae I–VII (23, 24), neurons with mixed synapses in those laminae were identified as interneurons (eight examples). Likewise, large-diameter (i.e., >40 μm) neurons with mixed synapses in laminae VIII and IX were identified as motor neurons (two examples). (The remaining 22 neurons with mixed synapses were not identifiable.)

To compare the relative numbers of chemical and mixed synapses, all identified patches of neuronal plasma membranes >4 μm^2 were photographed at ×10,000 in four replicas from lumbosacral enlargements, four from cervical enlargements, and two from the thoracic region. More than 420 stereopair electron micrographs containing 3200 μm^2 of neuronal plasma membrane were evaluated. The total area of plasma membrane examined is thus equivalent to 4–8% of the somatic and proximal dendritic plasma membrane of a single medium-diameter neuron (35, 36). In that relatively small fractional-equivalent of 1 neuron, 24 mixed synapses were found, for an average of 1 mixed synapse per 133 μm^2 of somatic and proximal dendritic plasma membrane (or 300–600 mixed synapses per cell). Because there were 2.4 gap junctions per mixed synapse and 78 connexons per gap junction (Fig. 6), this average is also equivalent to 1 gap junction/55 μm^2 of plasma membrane and to 1.4 connexons/μm^2. Because additional gap junctions may not have been recognized because of an inappropriate local shadowing angle or limited depth of focus that precluded recognition of small gap junctions in low-magnification electron micrographs, we consider these data as establishing lower limits for the concentration of mixed synapses, gap junctions, and connexons in somatic and proximal dendritic plasma membranes of neurons in adult rat spinal cord.

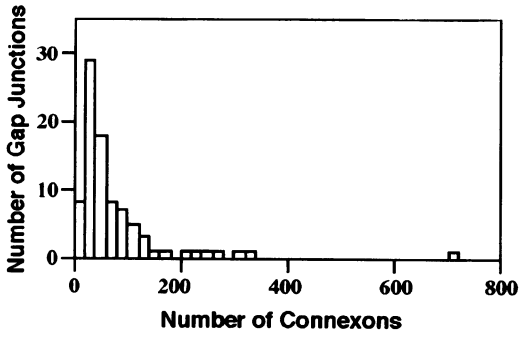

FIG. 6. Histogram depicting number of connexons (binned by 20) in each of 88 gap junctions. Median = 45 connexons; mean = 75.5 connexons; SEM = ±10.0 connexons; range = 6–704 connexons; skewness = 4.19.

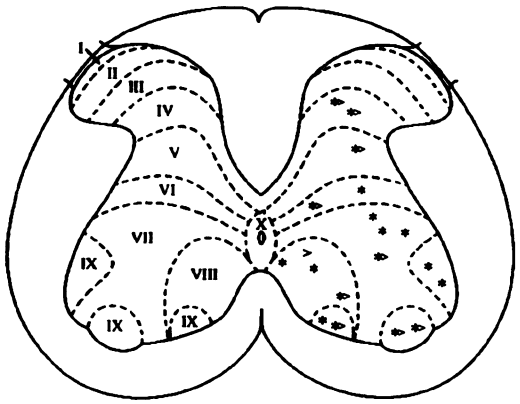

FIG. 7. Map of lumbosacral enlargement depicting gross anatomical and subcellular locations of 23 of 26 mixed synapses. (Two mixed synapses were not mapped, and two were on the same neuron. Locations of mixed synapses in thoracic and cervical cord are not shown.) *, soma; *>, proximal dendrite; >, small dendrite.

DISCUSSION

Mixed synapses are shown to be relatively abundant on neurons in the spinal cords of adult rats. Based on an estimated 40,000–80,000 μm^2 of somatic and proximal dendritic plasma membrane in motor neurons and interneurons (35, 36), the average value of 1 mixed synapse per 133 μm^2 of neuronal plasma membrane (all morphometric data combined) indicates that most neurons in the spinal cord have 300–600 mixed synapses (and 720–1440 gap junctions) on their somatic and proximal dendritic plasma membranes. (See Fig. 8 for diagrammatic representation of the concentration of mixed synapses on a typical neuron.) On an α-motor neuron, for example, 300–600 mixed synapses would constitute 3–12% of the estimated 5,000–10,000 synapses in the same area (35, 36). Of those 10,000 synapses, however, only 5–10% (or 500–1000) are thought to be excitatory, whereas 90–95% represent

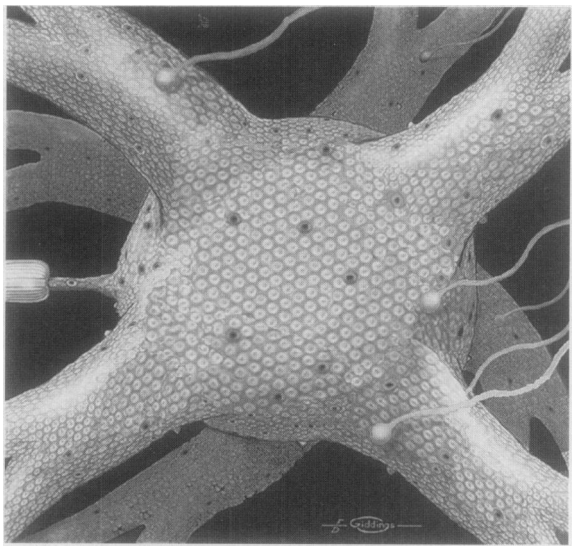

FIG. 8. Interpretive drawing of a typical spinal cord neuron with a portion of its 10,000 chemical synapses (clear ovals) and 300 mixed synapses (dark ovals) indicated on its somatic and proximal dendritic plasma membranes.

inhibitory synapses (35, 36). Moreover, ≈60% of inhibitory synapses contain flattened synaptic vesicles (33), whereas mixed synapses contained only spherical synaptic vesicles. Thus, if mixed synapses are excitatory and are present on α-motor neurons at the same density as on other neurons, 300–600 mixed synapses would constitute 30–100% of all their excitatory synapses.

Our data also indicate that mixed synapses are not restricted to a small population of neurons. For example, if all of the mixed synapses were restricted to 10% of all neurons, the average value calculated above would require that each member of that subset have 10 times as many mixed synapses (i.e., 3,000–10,000 on each somatic and proximal dendritic plasma membrane). Because no patches of plasma membrane were found where multiple (i.e., more than two) mixed synapses were present among as many as 12 other synapses, we conclude that most neurons in rat spinal cord have several hundred relatively widely scattered mixed synapses per cell (Fig. 8), rather than a small fraction of neurons having several thousand closely spaced mixed synapses.

Mixed synapses occur primarily on the electrically integrative portion of the cell—the soma and proximal dendrites. However, the small number of connexons and the limited electrical conduction at a single mixed synapse would be unlikely to cause electrical synchronization of neuron groups (37). Likewise, the intercellular geometry (38) at mixed synapses appears to preclude a dominant role for these extremely small gap junctions in conventional orthodromic electrical transmission in mammals (ref. 37, and see refs. 18 and 19), and would minimize detection of very small gap junctions on large neuronal somata using conventional intracellular recording and dye-transfer techniques (39). Consequently, only grid-mapped freeze-fracture techniques have the resolution and sensitivity to provide unambiguous evidence for the existence and distribution of very small gap junctions at mixed synapses in spinal cord neurons.

Although the electrical effects of mixed synapses have yet to be detected in adult mammalian spinal cord neurons using current electrophysiological methods (15, 17, 18), the presence of several small gap junctions at mixed synapses may, nevertheless, produce profound effects on the electrical and metabolic properties of coupled cells: (*i*) summation of electrical and chemical transmission would increase the amplitude of postsynaptic depolarization, thereby improving synaptic efficacy at excitatory synapses (37); (*ii*) retrograde electrical activation could potentiate neurotransmission in a particular subset of excitatory synapses, thereby providing a mechanism for recruitment of that class of excitatory fibers; (*iii*) retrograde activation of inhibitory terminals could provide a mechanism for negative-feedback inhibition; and (*iv*) direct transfer of metabolites and second messengers could be involved in regulation of synaptic efficacy (37) and/or defining functional groups of neurons [e.g., defining "pattern generator" circuits (40)].

The demonstration of abundant mixed synapses throughout the spinal cords of adult rats, where previously only chemical synapses were thought to occur, requires significant reassessment of our concepts of neuronal communication in the spinal cord, and perhaps in the entire central nervous system (5). Rather than the strictly unidirectional synaptic communication that was previously believed to occur, mixed synapses appear to provide abundant pathways for both metabolic coupling (41) and bidirectional synaptic communication between neurons in this major subdivision of the mammalian central nervous system.

We thank F. E. Dudek, D. S. Faber, P. Micevych, J. W. Walrond, and G. Zampighi for critical review of the manuscript. This work was supported by National Institutes of Health Grants NS31027 and S10 RR08329 (to J.E.R.) and by the College Research Council.

1. Korn, H., Sotelo, C. & Crepel, F. (1973) *Exp. Brain Res.* **16,** 255–275.
2. Sotelo, C. & Korn, H. (1978) *Int. Rev. Cytol.* **55,** 67–104.
3. Peters, A., Palay, S. L. & Webster, H. D. (1991) *The Fine Structure of the Nervous System: Neurons and Their Supporting Cells* (Oxford Univ. Press, New York), pp. 1–494.
4. Shapovalov, A. I. & Shiriaev, B. I. (1978) *Exp. Brain Res.* **33,** 313–323.
5. Sloper, J. J. (1972) *Brain Res.* **44,** 641–646.
6. Shepherd, G. M. (1988) in *Neurobiology*, ed. Shepherd, G. M. (Oxford Univ. Press, New York), pp. 65–86.
7. Bennett, M. V. L., Aljure, E., Nakajima, Y. & Pappas, G. D. (1963) *Science* **141,** 262–264.
8. Grinnell, A. D. (1970) *J. Physiol. (London)* **210,** 17–43.
9. Fulton, B. P., Miledi, R. & Takahashi, T. (1980) *Proc. R. Soc. London B* **206,** 115–120.
10. Bellinger, D. L. & Anderson, W. J. (1987) *Dev. Brain Res.* **35,** 69–82.
11. Walton, K. D. & Navarette, R. (1991) *J. Physiol. (London)* **433,** 283–305.
12. Matsumoto, A., Arnold, A. P., Zampighi, G. & Micevych, P. E. (1988) *J. Neurosci.* **8,** 4177–4138.
13. Matsumoto, A., Arnold, A. P. & Micevych, P. E. (1989) *Brain Res.* **495,** 362–366.
14. Dermietzel, R. & Spray, D. C. (1993) *Trends Neurosci.* **16,** 186–192.
15. Nelson, P. G. (1966) *J. Neurophysiol.* **29,** 275–287.
16. Llinas, R., Baker, R. & Sotelo, C. (1974) *J. Neurophysiol.* **37,** 560–571.
17. Werman, R. & Carlen, P. L. (1976) *Brain Res.* **112,** 395–401.
18. Gogan, P., Gueritaud, J. P., Horcholle-Bossavit, G. & Tyc-Dumont, S. (1977) *J. Physiol. (London)* **272,** 755–767.
19. Arasaki, K., Kudo, N. & Nakanishi, T. (1984) *Exp. Brain Res.* **54,** 437–445.
20. Rash, J. E., Dillman, R. K. Morita, M., Whalen, L. R., Guthrie, P. B., Fay-Guthrie, D. & Wheeler, D. W. (1995) in *Techniques in Biological Microscopy and Analysis*, eds. Severs, N. J. & Shotton, D. M. (Wiley–Liss, New York), pp. 127–150.
21. Hudson, C. S., Rash, J. E. & Shinowara, N. (1981) in *Current Trends in Morphological Techniques*, ed. Johnson, J. E. (CRC, Boca Raton, FL), Vol. 2, pp. 183–217.
22. Rash, J. E. & Yasumura, T. (1992) *J. Electron Microsc. Technol.* **20,** 187–204.
23. Rexed, B. (1954) *J. Comp. Neurol.* **100,** 297–379.
24. Brichta, A. M. & Grant, G. (1985) in *The Rat Nervous System*, ed. Paxinos, G. (Academic, Orlando, FL), Vol. 2, pp. 293–301.
25. Landis, D. M. D. & Reese, T. S. (1974) *J. Comp. Neurol.* **60,** 316–320.
26. Hatton, J. D. & Ellisman, M. H. (1981) *Cell Tissue Res.* **215,** 309–323.
27. Heuser, J. E., Reese, T. S., Dennis, M. J., Jan, Y., Jan, L. & Evans, L. (1979) *J. Cell Biol.* **81,** 275–300.
28. Miller, T. M. & Heuser, J. E. (1984) *J. Cell Biol.* **98,** 685–698.
29. Rash, J. E., Walrond, J. P. & Morita, M. (1988) *J. Electron Microsc. Technol.* **10,** 153–185.
30. Gulley, R. L. & Wood, R. L. (1971) *Tissue Cell* **3,** 675–690.
31. Revel, J. P. & Karnovsky, M. J. (1967) *J. Cell Biol.* **33,** C7–C12.
32. Branton, D., Bullivant, S., Gilula, N. B., Karnovsky, M. J., Moor, H., Northcote, D. H., Packer, L., Satir, B., Satir, P., Speth, V., Staehelin, L. A., Steere, R. L. & Weinstein, R. S. (1975) *Science* **190,** 54–56.
33. Brannstrom, T. (1993) *J. Comp. Neurol.* **330,** 439–454.
34. Larsen, W. J. (1983) *Tissue Cell* **15,** 645–671.
35. Eccles, J. C. (1957) *The Physiology of Nerve Cells* (Johns Hopkins Univ. Press, Baltimore), pp. 1–29.
36. Kandel, E. R., Schwartz, J. H. & Jessell, T. M. (1992) *Principles of Neural Science* (Elsevier, New York), pp. 18–43.
37. Pareda, A. E., Nairn, A. C., Wolszon, L. R. & Faber, D. S. (1994) *J. Neurosci.* **14,** 3704–3712.
38. Martin, A. R. & Pilar, G. (1963) *J. Physiol. (London)* **168,** 464–475.
39. Dudek, F. E. & Snow, R. W. (1985) in *Gap Junctions*, eds. Bennett, M. V. L. & Spray, D C. (Cold Spring Harbor Lab. Press, Plainview, NY), pp. 325–336.
40. Frank, E. & Mendelson, B. (1990) *J. Neurobiol.* **21,** 33–50.
41. Gilula, N. B., Reeves, O. R. & Steinbach, A. (1972) *Nature (London)* **235,** 262–265.